Local Segment Model for Elasto-Plastic Analysis of RPV Lower Head

Jang Min Park [a*], Kukhee Lim [b]
[a]*Yeungnam University, Daehak-ro 280, Gyeongsan 38541, Republic of Korea*
[b]*Korea Institute of Nuclear Safety, Gwahak-ro 62, Daejeon 341142, Republic of Korea*
[*]*Corresponding author: jpark@yu.ac.kr*

Keywords : severe accident, lower head failure, simplified model, elasto-plastic

1. Introduction

Under severe accident conditions in a nuclear power plant, the reactor pressure vessel (RPV) lower head is subjected to a significant thermal load from the corium. In addition, the lower head undergoes mechanical loads due to internal pressure of the vessel and the weight of the corium. These thermo-mechanical loads expose the lower head to a risk of failure.

Regarding the lower head failure assessment, stress calculation is an essential part of the modeling process. In severe accident codes (SACs), the stress is commonly calculated using simplified models [1]. The representative model is the pressurized vessel model, in which the stress state is represented in terms of effective stress, calculated by considering the balance with mechanical loads. The effect of the thermal gradient through the wall can be taken into account, thereby providing insight into the distribution of the effective stress through the wall. This model benefits from computational efficiency, yet it falls short in describing the detailed aspects of the stress state, particularly when the deformation is large and the lower head shape deviates significantly from a hemisphere.

This study aims to develop a simplified model for analyzing elasto-plastic deformation of the lower head under severe accident conditions. Specifically, the model treats a local segment of the lower head as a three-dimensional rectangular column, considering three normal components of stress and strain, while disregarding both shear and bending effects. On the boundary of the segment, the mechanical loading is treated as surface normal stresses. In this sense, the proposed model can be regarded as a three-dimensional extension of the effective stress model. This approach is named the Local Segment Model (LSM) in this study. The analysis begins with the elastic deformation of the LSM, which is then extended to include elasto-plastic deformation. To verify the LSM, the results are compared with those from finite element analysis (FEA).

2. Model Development

Fig. 1 shows section views of the RPV lower head. The lower head has a hemispherical shape with a uniform wall thickness denoted as e. Under severe accident conditions, the inner wall is subjected to thermal and mechanical loads, whereas the outer wall can be cooled by flooding the reactor cavity. Though not depicted in Fig. 1, gravitational force from the weight of corium and lower head is present. The segment is assumed as a rectangular column, while geometrical curvature of the lower head is considered only through the relationship between the internal pressure and the hoop stress. With the assumption in mind, we propose the Local Segment Model (LSM), which is depicted in Fig. 2. The coordinate system embedded in the segment is defined as follows: x represents the tangential direction, y the thickness-wise direction, and z the circumferential direction which is normal to xy-plane.

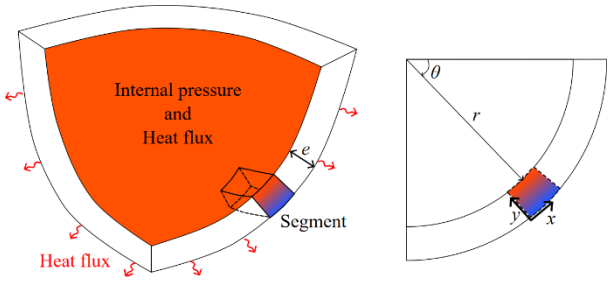

Fig. 1. Schematics of the RPV lower head and a local segment.

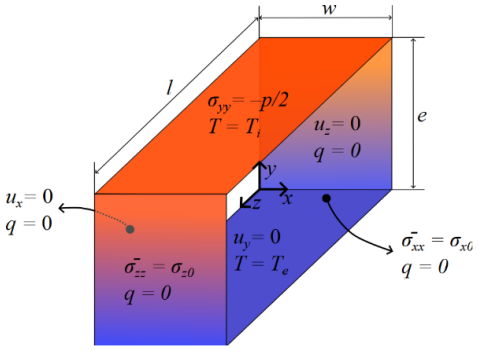

Fig. 2. A schematic of the Local Segment Model of the RPV lower head.

2.1 Local Segment

Major interest of the LSM is the elasto-plastic analysis of the lower head, and the details will be presented. The thermal analysis, on the other hand, will be conducted in a relatively simple manner.

For the thermal analysis in this study, we assume steady-state condition and neglect non-linearity due to

the temperature-dependent physical properties. Therefore, the temperature is assumed as a function of y as follows:

$$T(y) = A_1 + \frac{A_2}{r_e - y}, \quad (1)$$

where r_e is ex-vessel radius, and A_1 and A_2 are constants determined by the boundary conditions.

For the structural analysis, several assumptions are introduced to simplify the momentum conservation equation. Considering axis-symmetry of the domain, shear strain with respect to the z-direction should be zero. In addition, we neglect shear strain in xy-plane as well. This shear-free assumption has been implicitly adopted in the previous studies on the simplified modeling [1,2]. Under this condition, all shear stress components vanish.

We also neglect the gravitational body force. Thermal expansion is also not considered, since it has only minor effects on the lower head failure. The inertial effect is generally not taken into account in the SACs. It should be noted that in LSM model, the geometrical curvature is neglected, which will greatly simplify the upcoming analysis.

With the assumptions mentioned above, the momentum conservation equation can be simplified as follows:

$$\frac{d\sigma_{xx}}{dx} = 0, \frac{d\sigma_{yy}}{dy} = 0, \frac{d\sigma_{zz}}{dz} = 0. \quad (2)$$

To avoid rigid body motion of the segment, we set constraints as follows:

$$u_x = 0 \text{ at } x = 0, \quad (3)$$

$$u_y = 0 \text{ at } y = 0, \quad (4)$$

$$u_z = 0 \text{ at } z = 0. \quad (5)$$

The mechanical loads are applied as follows:

$$\frac{1}{e}\int_0^e \sigma_{xx} dy = \sigma_{x0} \text{ at } x = w, \quad (6)$$

$$\sigma_{yy} = -\frac{p}{2} \text{ at } y = e, \quad (7)$$

$$\frac{1}{e}\int_0^e \sigma_{zz} dy = \sigma_{z0} \text{ at } z = l. \quad (8)$$

The boundary conditions are depicted in Fig. 2.

2.2 Elastic Model

The elastic constitutive equation is written as follows:

$$\sigma = \lambda \mathrm{tr}(\varepsilon) I + 2\mu\varepsilon, \quad (9)$$

where λ and μ are Lamé parameters. Substituting the constitutive equation into the momentum conservation equations, Eq. (2), results in:

$$\frac{\partial^2 u_x}{\partial x^2} = 0, \quad (10)$$

$$(\lambda + 2\mu)\frac{\partial^2 u_y}{\partial y^2} + \left(\frac{\partial \lambda}{\partial y} + 2\frac{\partial \mu}{\partial y}\right)\frac{\partial u_y}{\partial y} + \frac{\partial \lambda}{\partial y}\left(\frac{\partial u_x}{\partial x} + \frac{\partial u_z}{\partial z}\right) = 0, \quad (11)$$

$$\frac{\partial^2 u_z}{\partial z^2} = 0. \quad (12)$$

The momentum equation along with the boundary conditions undergo further mathematical manipulation resulting in a linear equation. Finally, the elastic deformation and stress are obtained by solving the linear system numerically.

2.3 Elastic-Perfectly Plastic Model

Assuming that hardening is negligible, $\sigma_{eq} = \sigma_Y$ in the yielded region where σ_Y is the yield stress. In other words, von Mises yield criterion in the LSM model is written as follows:

$$\sqrt{\frac{1}{2}\left(\left(\sigma_{xx} - \sigma_{yy}\right)^2 + \left(\sigma_{yy} - \sigma_{zz}\right)^2 + (\sigma_{zz} - \sigma_{xx})^2\right)} = \sigma_Y. \quad (13)$$

An iterative method is used to find σ_{xx} and σ_{zz}, which is schematically described in Fig. 3. The stress field, computed from the elastic model, is taken as the initial guess. The yield criterion of Eq. (13) is then applied to yielded region, while the elastic model is applied to unyielded region. At this moment, we assume for simplicity that $\sigma_{zz} = \alpha\sigma_{xx}\$$ in the yielded region, where $\alpha = \frac{\sigma_{z0}}{\sigma_{x0}}$. Then, the yield criterion is rewritten as a quadratic equation for σ_{xx} as follows:

$$(\alpha^2 - \alpha + 1)\sigma_{xx}^2 - \sigma_{yy}(1 + \alpha)\sigma_{xx} + \sigma_{yy}^2 - \sigma_Y^2 = 0\ , \quad (14)$$

and the roots can be found analytically. Among the two roots, we take the larger one corresponding to tensile loading in x-direction. The stress and yielded region are then updated until convergence.

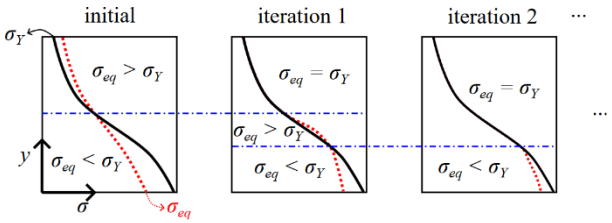

Fig. 3. A schematic description of the iteration method to compute the stress of elastic-perfectly plastic model. The dash-dot line indicates the yield surface, which is updated after each iteration.

3. Results

We consider a hemispherical lower head made of SA533B1 steel [3,4]. The lower head is under internal pressure and thermal load as shown in Fig. 1. The thermal load is imposed by specifying the in- and ex-vessel temperatures. The pressure and thermal loads can vary with time in general, but in this study, they are assumed to remain constant. We will compare the LSM with the finite element analysis (FEA) under four specific test conditions. This comparison will clarify the model's performance in stress prediction and identify its limitations. The FEA is conducted using an open source software Code-Aster, and the performance had been validated in the previous study [5].

Four different test cases are considered, with the parameters summarized in Table 1. The average radius is fixed at 0.465 m, while the wall thickness is varied. The internal pressure is selected such that the effective stress, $\sigma_{eff} = \frac{pr_i^2}{r_e^2 - r_i^2}$, remains constant at 72.58 MPa. The ex-vessel wall temperature is set at 500 K, whereas

the in-vessel wall temperature is varied. These parameters align with the range of experimental conditions of LHF and OLHF tests.

We first present the results of the elastic model. Fig. 4 shows the stress and temperature profiles along the thickness for cases A1 and A2. In case A1, which has a thinner wall, the results generally match between LSM and FEA. This agreement suggests that the stress distribution along the thickness is dominated by the nonlinearity due to the thermal gradient in this particular case, rather than the geometrical curvature effect.

As the thickness is increased in case A2, a larger discrepancy in the stress is observed, especially near the ex-vessel wall. The discrepancy reflects a limitation of LSM due to the assumption neglecting the geometrical curvature effect.

Fig. 5 shows the results for cases B1 and B2. Compared to previous cases A1 and A2, the in-vessel temperature is increased to 1500 K, significantly lowering the elastic modulus near the in-vessel wall. Under such conditions, the region near the in-vessel wall nearly does not support the tensile load. In other words, σ_{xx} in $y/e > 0.8$ is almost negligible. As the wall thickness is increased in Fig. 5(b), σ_{xx} even becomes negative near the in-vessel wall. This indicates that the deformation near the in-vessel wall is primarily driven by compression in the radial direction (y-direction), rather than extension in the circumferential or tangential direction.

In general, LSM and FEA results agree regarding the elastic deformation for the test cases considered. Particularly for case B2, the equivalent stress and yield stress are shown in Fig. 6(a). It can be found that $\sigma_{eq} > \sigma_Y$ near the in-vessel wall, indicating the yielding. Other cases do not involve yielding and the results are not shown. Therefore, elasto-plastic analysis is conducted for case B2, and the results are shown in Fig. 6(b). The equivalent stress, indicates that LSM can capture the yielded region similarly to FEA. However, consideration of the yielding does not significantly affect the stress profile in this particular case.

Table I: Test case parameters.

Case	Wall Thickness (mm)	Internal Pressure (MPa)	In-vessel Temperature (K)
A1	30	10	1000
A2	90	34.44	1000
B1	30	10	1500
B2	90	34.44	1500

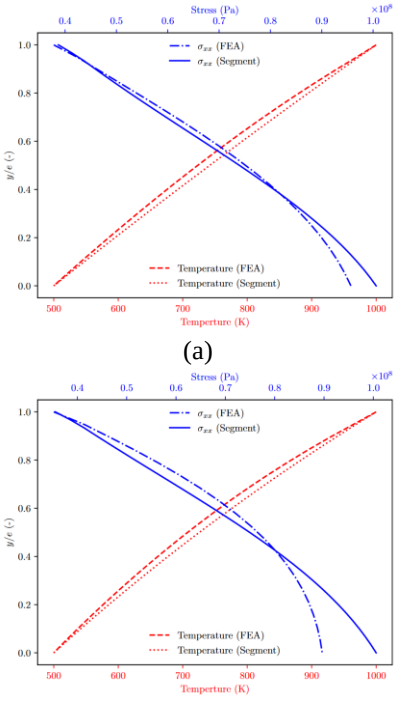

(a)

(b)

Fig. 4. Stress, σ_{xx}, and temperature profiles for (a) Case A1 and (b) Case A2 with elastic model.

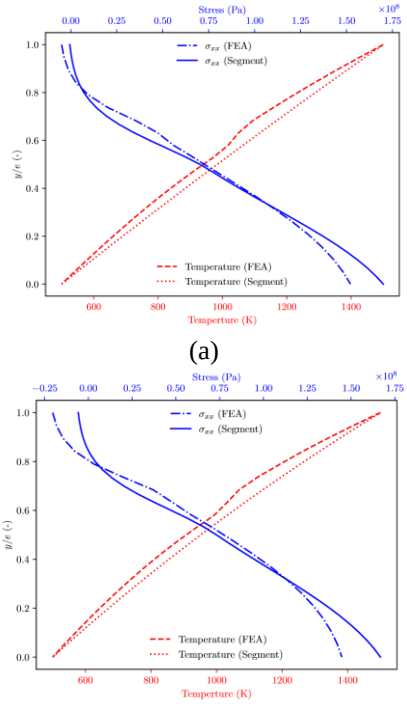

(a)

(b)

Fig. 5. Stress, σ_{xx}, and temperature profiles for (a) Case B1 and (b) Case B2 with elastic model.

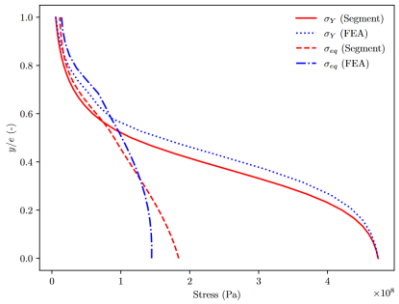

(a)

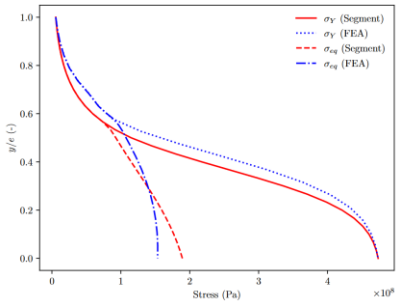

(b)

Fig. 6. Equivalent stress and yield stress profiles for Case B2 with (a) elastic model and (b) elastic-perfectly plastic model.

4. Conclusions

This study proposes a simplified model which assumes a local segment of the reactor pressure vessel's lower head as a three-dimensional rectangular column. The model considers three normal components of both stress and strain, while shear effects and bending moments are neglected. The model is applied to both elastic and elasto-plastic analysis of the lower head, and the results are compared with those from FEA for verification. Generally, the model and FEA show good agreement, although deviations increase with wall thickness. The model also effectively captures the yielded region, similarly to FEA.

ACKNOWLEDGEMENT

This work was supported by the Nuclear Safety Research Program through the Korea Foundation Of Nuclear Safety (KoFONS) using the financial resource granted by the Nuclear Safety and Security Commission (NSSC) of the Republic of Korea. (No. 2106007).

REFERENCES

[1] L. L. Humphries, B. A. Beeny, F. Gelbard, T. Haskin, D. Louie, J. Phillips, J. Reynolds, R. C. Schmidt, and S. Campbell. MELCOR Computer Code Manuals Vol. 2: Reference Manual Version 2.2 r2023.0, 2023.
[2] V. Koundy and I. Cormeau. Semi-analytical modeling of a PWR lower head failure under severe accident conditions using an axisymetrical shell theory. Nuclear Engineering and Design, Vol. 235, p. 845, 2005.
[3] T.Y. Chu, M.M. Pilch, J.H. Bentz, J.S. Ludwigsen, W.-Y. Lu, and L.L. Humphries. Lower Head Failure Experiments and Analyses, NUREG/CR-5582, 1999.
[4] L.L. Humphries, T.Y. Chu, J. Bentz, R. Simpson, C. Hanks, W. Lu, B. Antoun, C. Robino, J. Puskar, and P. Mongabure. OECD Lower Head Failure Project Final Report, 2002.
[5] J.M. Park and K. Lim. Multi-dimensional finite element analyses of OECD lower head failure tests. Nuclear Engineering and Technology, Vol. 54, p. 4522, 2022